Princeton Plasma Physics Laboratory

PPPL-4191
PPPL-4191

Edge Turbulence Measurements in Toroidal Fusion Devices

S.J. Zweben, J.A. Boedo, O. Grulke, C. Hidalgo,
B. LaBombard, R.J. Maqueda, P. Scarin, and J.L. Terry

November 2006

PPPL
PRINCETON PLASMA
PHYSICS LABORATORY

Prepared for the U.S. Department of Energy under Contract DE-AC02-76CH03073.

Princeton Plasma Physics Laboratory
Report Disclaimers

Full Legal Disclaimer

This report was prepared as an account of work sponsored by an agency of the United States Government. Neither the United States Government nor any agency thereof, nor any of their employees, nor any of their contractors, subcontractors or their employees, makes any warranty, express or implied, or assumes any legal liability or responsibility for the accuracy, completeness, or any third party's use or the results of such use of any information, apparatus, product, or process disclosed, or represents that its use would not infringe privately owned rights. Reference herein to any specific commercial product, process, or service by trade name, trademark, manufacturer, or otherwise, does not necessarily constitute or imply its endorsement, recommendation, or favoring by the United States Government or any agency thereof or its contractors or subcontractors. The views and opinions of authors expressed herein do not necessarily state or reflect those of the United States Government or any agency thereof.

Trademark Disclaimer

Reference herein to any specific commercial product, process, or service by trade name, trademark, manufacturer, or otherwise, does not necessarily constitute or imply its endorsement, recommendation, or favoring by the United States Government or any agency thereof or its contractors or subcontractors.

PPPL Report Availability

Princeton Plasma Physics Laboratory:

http://www.pppl.gov/pub_report/

Office of Scientific and Technical Information (OSTI):

http://www.osti.gov/bridge

U.S. Department of Energy:

U.S. Department of Energy
Office of Scientific and Technical Information
P.O. Box 62
Oak Ridge, TN 37831-0062
Telephone: (865) 576-8401
Fax: (865) 576-5728
E-mail: reports@adonis.osti.gov

Edge Turbulence Measurements in Toroidal Fusion Devices

S.J. Zweben[1], J.A. Boedo[2], O. Grulke[3], C. Hidalgo[4],
B. LaBombard[5], R.J. Maqueda[6], P. Scarin[7], J.L. Terry[5]

[1] *Princeton Plasma Physics Laboratory, Princeton, NJ USA*
[2] *University of California at San Diego, San Diego, CA USA*
[3] *MPI for Plasma Physics, Euratom Association, Greifswald, Germany*
[4] *Laboratorio Nacional de Fusión, CIEMAT, Madrid, Spain*
[5] *Massachusetts Institute of Technology, Cambridge MA USA*
[6] *Nova Photonics, Inc. Princeton NJ USA*
[7] *Associazione Euratom-ENEA sulla Fusione, Padova, Italy*

Abstract

This paper reviews measurements of edge plasma turbulence in toroidal magnetic fusion devices with an emphasis on recent results in tokamaks. The dominant feature of edge turbulence is a high level of broadband density fluctuations with a relative amplitude $\delta n/n \sim 5$-100%, accompanied by large potential and electron temperature fluctuations. The frequency range of this turbulence is ~10 kHz-1 MHz, and the size scale is typically ~0.1-10 cm perpendicular to the magnetic field but many meters along the magnetic field, i.e. the structure is nearly that of 2-D 'filaments'. Diagnostic and data analysis techniques are reviewed and the main experimental results are summarized. Recent comparisons of experimental results with edge turbulence theory are discussed, and some directions for future experiments are suggested.

1. Introduction

The edge plasma in toroidal magnetic fusion devices is important because it determines the interaction between the plasma and the first-wall and/or divertor structures. In particular, the radial cross-field transport through the edge plasma strongly influences the location and strength of the heat and particle flux to the wall, as well as the processes of recycling, impurity influx, and He ash removal. The edge plasma also sets the boundary condition for the confined plasma, and so can also affect the global confinement (as in the H-mode). Thus an understanding of the cross-field transport process in the edge plasma is crucially important for creating a magnetic fusion reactor.

It has been recognized for many years that the cross-field plasma transport through the edge is dominated by turbulence. The basic characteristics of edge turbulence are fairly universal, as discussed in previous reviews of experimental results [1-8]. The theory of edge turbulence which is necessary for understanding these results has also evolved over many years, but will not be covered in this paper except in the context of specific experimental results.

Edge turbulence dominantly consists of broadband plasma density fluctuations with a fluctuation amplitude $\delta n/n \sim 5\text{-}100\%$, with relative fluctuation levels typically increasing toward the first wall. Associated with these density fluctuations are also potential and electron temperature fluctuations of similar relative magnitude, and considerably smaller magnetic fluctuations. The observed frequency range is typically $f \sim 10$ kHz

to 1 MHz with a broad spectrum, i.e. with an autocorrelation time in the range of 10's of microseconds. The size scales perpendicular to the magnetic field are within the range $L_{\perp}$~0.1-10 cm, but the size scale along the magnetic field direction is typically 10's of meters, i.e. the structure is nearly that of 2-D 'filaments'. These density fluctuations have often been identified with drift waves, but the observed fluctuations are clearly not linear instabilities since they have a broadband frequency spectrum which persists for times much longer than a typical linear growth time. In fact, the structure of edge turbulence is often highly intermittent and not at all like that of linear instabilities.

This paper will review some of the measurements of edge turbulence obtained over the past 30 years on toroidal magnetic fusion devices, i.e. tokamaks, stellarators, and reversed field pinches (RFPs), with an emphasis on tokamaks (which seem to be the best candidate for a magnetic fusion reactor). First there is a brief history of this subject (Sec. 2), then a survey of diagnostics (Sec. 3) and data analysis methods (Sec. 4). The main body of the paper summarizes the experimental results on selected topics with representative examples (Sec. 5). The paper concludes with a discussion , which includes a comparison with non-fusion devices and with theory, and directions for further research (Sec. 6).

2. Brief History

Measurements of plasma turbulence have been made for well over 30 years. A few highlights of this history are summarized below.

One of the earliest of studies of magnetized plasma turbulence was done on the 'calutron' isotope separation process during the Manhattan Project [9]. In addition to presenting the famous Bohm diffusion formula (Chapter 2), Bohm et al described plasma 'hash', or broadband density fluctuations in the frequency range ~ 1 kHz-1 MHz (Chapter 9), as observed with Langmuir probes in these arc plasmas ($n \sim 3x10^{13}$ cm^{-3}, $T_e \sim$ 5-10 eV, $B \leq 12$ kG). Bohm et al clearly understood the role of turbulent electric fields in cross-field transport, but could not establish a quantitative connection between the turbulence and the transport.

Plasma turbulence was measured in many early magnetic fusion devices. According to Nedospasov [10], edge turbulence was measured on the first tokamak TMP at Kurchatov in 1956. Chen [11] noted the apparent universality of the turbulence frequency spectrum and tried to explain the power law fall-off on the basis of drift-wave theory. Detailed probe studies of large-scale coherent edge density fluctuations were done on the C-Stellarator at Princeton, including a direct measurement of the fluctuation-induced radial ExB transport [12]. The 3-D structure of both edge density and magnetic field turbulence was measured on the Zeta reversed field pinch (RFP) device at Culham [13], and was described as 'a system of convective rolls aligned along the magnetic field'. These early measurements are at least qualitatively similar those in present devices, although they were made using analog techniques. Digital signal processing for turbulence and ExB transport analysis was introduced by Powers in the mid-1970's [14].

Since the late-1970's there has been a sustained effort to measure and understand plasma turbulence at the edge of toroidal fusion devices. The main motivation for this work was to clarify the cross-field plasma transport mechanism which determines the plasma-wall interaction. A second motivation was to understand physics of plasma turbulence, e.g. the origin of the H-mode. The distinction between the core and the edge is not a sharp one: roughly, the edge is the region outside r/a ~ 0.9 where T_e ~ 10-100 eV, including the whole region from the last closed flux surface to the first wall, i.e. the "scrape-off layer" (SOL), but not including (for the purposes of this review) the H-mode pedestal, which can reach $T_e \leq 1$ keV.

3. Diagnostic Methods

Experimental studies of neutral gases and liquids have shown that it is necessary to measure a wide range of space and time scales to understand the turbulent velocity fields [15]. Characterizing plasma turbulence is more difficult since there are many fluctuating quantities of interest, such as the electron density n, electron and ion temperatures T_e and T_i, electrostatic potential ϕ, magnetic field **B**, and flow speed **v**. For edge turbulence the main quantities of interest are n, T_e, ϕ (from which the ExB drift velocity can be inferred), and **B**.

There are several standard methods for measuring these edge plasma fluctuations in tokamaks and similar devices; namely, electric and magnetic probes, laser scattering, microwave reflectometry, optical imaging, and

heavy ion beam probes. These have been summarized in previous reviews and books [3,16-21], so here only a brief summary of the advantages and limitations of each method is presented. Some additional possibilities are discussed in Sec. 6.3.

3.1 Electric and magnetic probes

Electric (a.k.a. Langmuir) and magnetic field probes have been used to measure fluctuations in plasmas since the earliest magnetic fusion devices. The technique is simply to insert one or more small biased electrodes or magnetic pickup coils inside the plasma, and then measure the frequency and wave number spectra of the fluctuations seen by these probes. Probe signals contain a large amount of data which can be interpreted in terms of the local n, T_e, ϕ, or **B** within the frequency and size scales of interest, i.e. f ~ 10 kHz-1 MHz and $L_\perp$ ~ 0.1-10 cm.

The biggest limitation of probes is that they can only be used when they do not significantly perturb the plasma or *vice versa* . In practice, this allows plasmas with up to T_e~100 eV to be measured using a fast movable drive when necessary. The main uncertainty in the use of these probes is the (generally) unknown level of plasma perturbation which may be present, which can be caused by the local interruption of plasma flows or current or by recycling and impurity influx at the probe surface [22,23]. Nevertheless, probe measurements of density and temperature have often been successfully compared with non-perturbing measurements such as Thomson scattering.

3.2 Electromagnetic wave scattering

Electromagnetic wave scattering has been used to measure fusion plasma turbulence since the mid-1970's [24,25]. This method is non-perturbing but also non-local, i.e. the sampling volume is usually much larger than the turbulence correlation length, so it is difficult to obtain spatial resolution within the edge region. An advantage of this technique is that the k-spectrum can be directly measured by varying the scattering angle.

Edge turbulence in fusion devices has been measured using both CO_2 and FIR laser scattering. With FIR the "edge" scattering volume also includes a significant region of the core plasma [e.g. 26], and with CO_2 the scattering volume is a generally a chord through the plasma [e.g. 27]. However, information about k-spectra can be obtained if the spatial localization of the turbulence is known, e.g. through improved spatial localization using crossed-beam correlation techniques [28, 29]. Some information on edge turbulence can also be obtained from chord-averaged density fluctuation measurements, e.g. phase contrast imaging (PCI) [30].

3.3 Microwave reflectometry

Microwave reflectometry has often been used to measure edge turbulence [16,17]. However, the interpretation of the signal in terms of the local turbulent density fluctuations is not straightforward, particularly when the relative fluctuation level is high, as it usually is in the edge plasma [31]. Nevertheless, much data has been obtained and qualitative interpretations of it have been presented, e.g. concerning the L-H transition in DIII-D [32].

Good agreement between reflectometer and Langmuir probe fluctuation measurements was found at CCT and DIII-D [33].

Recent improvements in this technique include 2-beam correlation reflectometry for measuring radial correlation lengths [34,35], Doppler reflectometry for measuring zonal flows [36], and methods for estimating radial and poloidal wave number spectrum [37,38]. In each case some assumptions are needed in order to interpret the results in terms of the local edge density fluctuations. Alternatively, the characteristics of the wave scattering process can be added to the theoretical turbulence model in order to compare the theory with the measurements [39].

3.4 Optical line emission

The visible line emission from neutral atoms in the plasma edge can be used to measure the space/time structure of edge turbulence. Passive visible imaging of edge turbulence has been done for many years [40,41]. More recently, 2-D imaging perpendicular to the main magnetic field was obtained by using beam emission spectroscopy (BES) or gas puff imaging (GPI) [42-49]. A close correlation between optical signals and Langmuir probe fluctuations has been observed at Caltech [50] and ASDEX [41].

The main advantage of this method is that a large number of spatial points can be sampled rapidly and simultaneously using discrete detectors or fast cameras. The main disadvantage is that the atomic physics of the line emission depends nonlinearly on the electron density (and the electron temperature in GPI) , so it is necessary to have an independent measurement

of the average n and/or T_e to directly estimate the actual density or temperature fluctuation level.

3.5 Heavy ion beam probe

A heavy ion beam probe injects a singly-ionized high energy beam into the plasma (e.g. Thallium at 500 keV) and detects the doubly-ionized ions which exit the plasma. The intersection of the probe and detected beams defines a small sampling volume which can be swept across the plasma. The detected beam current and potential can be used to simultaneously measure the local density and space potential with a time resolution sufficient to measure the turbulence and local ExB transport. However, these signals are very small and difficult to measure (e.g. a few volts compared the ~100 keV beam energy), and can be affected by fluctuations elsewhere along beam trajectory.

Edge turbulence measured with this method has shown edge density and potential fluctuation levels similar to those seen by Langmuir probes [51,52]. The presence of zonal flows can be detected by simultaneous changes in potential at different poloidal angles on a flux surface [53,54], and preliminary evidence for radially elongated 'streamers' was recently presented [55].

4. Data Analysis Methods

Most of the data analysis methods for plasma edge turbulence have

been used previously in other fields (e.g. fluid turbulence), and have also been described in previous diagnostic reviews (see Sec. 3), so only a brief summary of the advantages and limitations of each method is presented here.

4.1 Single-point time series

Standard analyses of single-point time series include estimates of the frequency spectrum, autocorrelation time, fluctuation levels, and probability distribution functions (PDFs) and higher order moments of the signals (e.g. skewness, kurtosis) [1-6]. Wave number spectra can be estimated from single-point time series by assuming "frozen flow' in one direction [56], even though flows can be at least 2-D in the edge plasma. Some recent examples of the use of these techniques can be found in [57].

Various other more specialized statistical techniques have been applied to edge turbulence data. Nonlinear couplings can be evaluated using bicoherence analysis [58-61]. Intermittent events (coherent structures) can be identified by various techniques [62-66]. Other statistical times series analyses include: fractal dimensionality [67,68], self-similarity [69-71], long-range correlations [72], and waiting or quiet time distributions [73-75]. Some of these methods require large data sets since they can be sensitive to infrequent events in the tail of the probability distribution function.

4.2 Two-point time series

Time series from two nearby sample volumes can be analyzed using the standard coherence function, from which the frequency-resolved

correlation coefficient and relative phase can be evaluated. These phases can be used to estimate the k-spectrum and the results can be presented as a (statistical) plot of the frequency vs. wave number. A phase velocity in the direction of separation can also be calculated, but its interpretation is ambiguous if the actual phase velocity also has a component in another direction, e.g. an artificial radial velocity could be inferred from a the poloidal motion of a 'tilted eddy' [76,77].

If the two measured points have a variable separation, the 2-D structure and motion of the turbulence can be estimated using the 'conditional sampling', or 'conditional averaging' technique [78-80]. This method generally identifies only features which are large amplitude (e.g. twice the standard deviation), and finds the time-averaged behavior over an ensemble of similar events.

4.3 Multipoint measurements and image analysis

Significantly more physical information can be obtained by making measurements at 3 or more points. For example, three nearby points are often used in order to evaluate the turbulence-induced ExB transport, two to measure the local potential fluctuations and one to measure the density fluctuations (see Sec. 5.9). Four probes are often used to estimate the Reynold's stress, two for each of the two electric field directions (see Sec. 5.8). Linear arrays can be used to directly measure the k-spectrum (see Secs. 5.3) and to look for asymmetry in the direction perpendicular to the main B field (see Sec. 5.4).

Image analysis of 2-D edge turbulence data from optical diagnostics has been used to identify 2-D turbulence flow fields in DIII-D [45,81-83] and the structure and motion of intermittent coherent structures or 'blobs' in Alcator C-Mod [84,85], TJ-II [86], and NSTX [46,87]. There is also a large literature in fluid mechanics on tracking and visualization of coherent structures [88].

4.4 Wavelet analysis of edge coherent structures

From the observations of bursts in single-point edge turbulence measurements a detailed analysis can be done to study the statistical properties of fluctuations at different time-scales $\tau=1/f$. By applying to these signals the Continuous Wavelet Transform (CWT), a set of wavelet coefficients $C_\tau(t)$ can be obtained for each time series; $C_\tau(t)$ represents the time behavior of characteristic fluctuations at each time-scale τ [89,90]. The statistical properties of bursts can be recognized from the PDFs [63,91,92] of the normalized wavelet coefficient fluctuations $\delta C_\tau/\sigma_\tau$ (σ_τ is the rms of $C_\tau(t)$). To quantify the weight of the tails with respect to the core of distribution, the scaling of flatness with τ has been considered. In the case of self-similar processes [93] the PDF of normalized fluctuation does not change its shape at different time scales. This reflects a constant flatness at all scales, whereas if the PDF of normalized fluctuations varies with a increasing of the tails of distribution at smaller scales the process is not self-similar and exhibits an intermittent character, implying an increase of flatness at smaller time scales.

5. Experimental results

There have been well over 300 experimental papers on edge turbulence measurements made on over 30 toroidal fusion devices since the late 1970's. This section will summarize the main experimental results with a few representative examples and mention counter-examples where appropriate. The theory of edge turbulence theory will not be discussed except in the context of specific edge turbulence measurements. Edge localized modes (ELMs) and other 'MHD' phenomena will not be discussed here.

Table 1 shows the typical range of edge plasma parameters for the experiments described in this section. Since many of the experimental results are common to many of the devices, some effort has been made to provide a diversity of references, and not every experimental paper in this field has been cited. Previous reviews can be consulted for further details and references [1-8].

Table 1: Range of Edge Plasma Parameters

$B(a) = 2\text{-}45$ kG (toroidal magnetic field)

$n_e(a) \approx 0.1\text{-}10 \times 10^{13}$ cm^{-3} (electron density)

$T_e(a) \approx 10\text{-}100$ eV (electron temperature)

$\rho_s \sim 0.01\text{–}0.2$ cm (ion gryoradius assuming $T_i=T_e$)

$\nu_{ei} \sim 10^5\text{–}10^7$ sec^{-1} (electron-ion collision frequency)

$\beta_e \sim 10^{-3}\text{-}10^{-5}$ (total edge beta)

1) Edge turbulence levels

The radial profiles of edge turbulence are fairly universal and similar to those shown in Fig. 1, which were made on Ohmic plasmas in the DIII-D tokamak using a movable Langmuir probe [94]. The radial profile of the electron density fluctuations typically increase from $\delta n/n \sim 5\%$ at a few cm inside the separatrix to $\delta n/n \leq 100\%$ in the far scrape-off layer (SOL), varying smoothly across the last closed magnetic surface. Qualitatively similar results were seen in NBI heated plasmas in DIII-D and in most other toroidal fusion devices, e.g. in TFTR tokamak [95], the ATF stellarator [96], and the RFX reversed field pinch [97].

The relative plasma potential fluctuation level normalized to T_e has a similar magnitude to $\delta n/n$, but does not necessarily follow the Boatman relation $\delta\varphi/T_e = \tilde{n}/n$, e.g. in TEXT [51] and in RFX [98]. The measurement of electron temperature fluctuations is difficult but generally shows $\delta T_{e/}T_e \sim$ (0.3-0.4) $\delta n/n$, e.g. in DIII-D [99], TEXT [100], the SINP tokamak [101], and the FTU tokamak [102]. In JET it was found that $\delta T_{e/}T_e \sim 0.1$ throughout the SOL [103]. In RFPs the edge electron temperature fluctuations show $\delta T_e/T_e \sim 0.5\ \delta n/n$ in the frequency range lower than 250 kHz [98], as obtained with triple Langmuir probe in RFX at low plasma current values. The same level was confirmed from measurement with helium line intensity ratios, at higher plasma current values, but limited to frequency range lower than 5 kHz [43].

There is also a small level of broadband edge magnetic turbulence in

tokamaks and stellarators of typically $\delta B_r/B_T \sim 10^{-5}$, increasing to $\delta B_r/B_T \sim 10^{-4}$ inside the last closed flux surface [104-106]. In RFPs the relative edge magnetic fluctuation levels are higher, i.e. $\delta B_r/B_T \sim 10^{-2}$ [107,108], but much of this is due to a superposition of many coherent global modes and not to small-scale turbulence.

A distinction is sometimes made between the 'near-SOL', which is located just outside the separatrix, and the 'far-SOL', which is located nearer to the wall [109,110]. The near-SOL is characterized by relatively large average gradients and near-Gaussian statistics, while the far-SOL can have nearly flat average gradients and strongly intermittent, convective transport.

2) Frequency spectra and phase velocity

The frequency spectrum of edge turbulence is generally flat up to some critical frequency in the range ~10-100 kHz, depending on the device, above which it falls like an inverse power law with exponent ~(1-4). This is illustrated in Fig. 2 by data taken with Langmuir probes on four devices [111]. In this figure the frequency spectra were 'rescaled', e.g. the JET tokamak frequencies were actually ~4.5 times lower than those in the TJ-I tokamak (which was not rescaled). This data was taken at radial positions where the poloidal phase velocity $V_{pol} \sim 0$, which generally occurs near (or the just inside) the last closed flux surface. Similar spectra have been seen on toroidal fusion devices since at least 1964 [112].

The phase velocity of the edge turbulence in the poloidal direction in a

tokamak [e.g. 51] or stellarator [e.g. 113] is typically $\leq 10^6$ cm/sec (in the lab frame), and generally changes sign from the electron diamagnetic drift direction inside the last closed flux surface to the ion diamagnetic drift direction in the SOL. The phase velocity in a RFP in the direction perpendicular to the magnetic field (and perpendicular to the minor radius) is in the toroidal direction, but behaves similarly [e.g. 114]. Thus there is a usually a relatively strong velocity 'shear layer' just inside the last closed flux surface, with or without a divertor or an H-mode.

The radial velocity of edge turbulence in tokamaks and stellarators is generally comparable to or smaller than to than the poloidal velocity near or inside the last closed flux surface, but the radial velocity can be larger than the poloidal velocity in the SOL, typically $\sim 10^5$ cm/sec (or $\sim$ 1% of the local sound speed). The radial velocity of intermittent objects slowed down with increasing radius in the SOL of DIII-D [62], but sometimes increased with minor radius in Alcator C-Mod [84]. The radial velocity is particularly important due to its relationship to the cross-field transport in the SOL (see Sec. 5. 9).

3) Spatial Structure

The spatial structure of edge turbulence generally consists of highly elongated 3-D 'filaments' with a size-scale much smaller than the plasma radius perpendicular to B but much longer than the plasma radius along B. Figure 3 shows an example of the perpendicular 2-D radial vs. poloidal structure of edge density turbulence as measured with GPI diagnostic on Alcator C-Mod [115]. Qualitatively similar 2-D images have been measured

on DIII-D [116], NSTX [117], and W7-AS [76].

Edge turbulence in tokamaks and stellarators has an spectrum-averaged poloidal correlation length $L_{pol} \sim 0.5$-5 cm and a radial correlation length $L_{rad} \sim(0.5\text{-}1)\ L_{pol}$, although the measurements on TEXTOR yielded $L_{rad} \sim(0.25\text{-}0.33)\ L_{pol}$ [118]. In RFPs the edge magnetic field is all poloidal so the turbulence structures are elongated filaments in the poloidal direction and move in that toroidal direction. The average toroidal correlation length is L_{tor}~10-20 cm with $L_{rad} \sim(0.2\text{-}0.4)\ L_{tor}$ [97,119].

Several measurements of the 1-D k-spectra have also been made, generally with 1-D probe arrays or multipoint optical techniques [42,115,120]. In tokamaks and stellarators, the shape of the k_{pol}-spectrum (integrated over frequency) is roughly similar to the shape of the frequency spectra (integrated over k_{pol}), as expected from a simple 'frozen flow' hypothesis. The shape of the k_{rad} spectrum in the edge is sometimes difficult to measure since the plasma parameters are often changing on a radial scale comparable to the radial correlation length.

The spatial scale of intermittent structures or 'blobs' is not necessarily the same as the spatial scale measured by the spectrum-averaged correlation length. The structure of intermittent objects in discussed in Sec. 5.6.

The parallel structure of the edge turbulence along the local magnetic field has been measured several times with Langmuir probes with the result that $L_{||} >> L_{\perp}$ [e.g. 76,121,122]. This structure is also seen in the nearly 2-D

filamentary structure of light emission from the edge [40,85,123], and is expected theoretically due to the rapid electron motion along B.

4) Poloidal variations

In limited (i.e. non-diverted) tokamaks, there is generally a similar relative fluctuation level on the high-field side and low-field side midplane, e.g. on the tokamaks CCT [124], CASTOR [125], and T-10 [126,127]. An up/down asymmetry of edge turbulence was reported in the limited tokamaks TEXT [26] and Tore Supra [128]. Recent measurements in the stellarator LHD showed an approximate up/down symmetry in the edge density fluctuations [129].

In diverted tokamaks, the relative fluctuation level at the inner midplane was seen to be about 10 times lower than that on the same flux surface at the outer midplane on Alcator C-Mod [115,130]. Measurements of electrostatic potential fluctuations near the X-point of the DIII-D divertor showed a reduced level compared with outer midplane and the upper (non-X-point) poloidal location [131], and a difference in intermittency was seen between the low-field and high-field sides of the divertor X-point in MAST [132]. Thus a significant poloidal asymmetry can occur in diverted tokamaks, probably dependent on the detailed magnetic topology.

It is not clear whether these asymmetries are due to the direct effect of limiters or divertors or to their indirect effects on the edge plasma parameters. However, it is clear that poloidal variations should be evaluated before drawing any conclusions concerning turbulent transport [133].

5) Plasma parameter scalings

The clearest scaling of edge turbulence for tokamaks and stellarators is for the poloidal size scale [e.g. 134]:

$$<k_{pol}>\rho_s \sim 0.02 - 0.1 \qquad [1]$$

where $<k_{pol}>$ is the average poloidal wave number and ρ_s is the local ion gyroradius (assuming $T_i=T_e$). The form of this scaling was motivated by simple theoretical models which predict the linear growth rate for drift waves to peak near $<k_{pol}>\rho_s \sim 0.3$. Most tokamaks and stellarators show this scaling [1-6], including recent results in DIII-D L-mode plasmas (for $r/a \leq 0.95$) [120] and the TJ-K torsatron [135]. Most of this scaling seems to be due to the inverse relationship between poloidal correlation length and toroidal magnetic field [41].

Another theory-based scaling is the 'mixing length' limit:

$$\delta n/n \sim 1/(k_{rad}\, L_n) \qquad [2]$$

at which point the fluctuations can flatten the average radial density gradient (where $L_n = n/(dn/dr)$). The evidence for this scaling comes mainly from the increase in the relative fluctuation level $\delta n/n$ with increasing minor radius, such as illustrated in Fig. 1. Density fluctuation levels were seen to scale vs. radius as $(\rho^*)^{1.4\pm0.4}$ in DIII-D [120]. However, systematic scans in TEXT did not see a variation of $\delta n/n$ with $\rho_s/L_{n,}$ as would be implied by Eqs. [1] and [2]

[134], and Eq. 2 is not consistent with the evidence for strong intermittency and convective transport in the SOL (see Sec. 5.6).

There have been a variety of empirical results on the scaling of edge turbulence with plasma density. The correlation lengths increased with line-averaged density in ASDEX [41], Alcator C-Mod [109], and TEXTOR [118]. However, the relative edge density fluctuation level was insensitive to the local edge density in the Caltech [136] and TEXT tokamaks [134]. The density of the intermittent events was linearly proportional to the edge plasma density in DIII-D L-modes [137]. An increase in SOL fluctuations in the 'near-SOL' was correlated with the density limit [109,138]. The edge turbulence was roughly independent of the plasma current and edge safety factor q(a) in the ASDEX and TEXT tokamaks [41,134], which is consistent with the similarity in edge turbulence of tokamaks, stellarators, and RFP's. A recent analysis of the cross-field fluxes in the near-SOL suggests a dependence on the collisionality and poloidal beta gradient [139].

For comparison with edge turbulence theory, it is natural to evaluate the scaling of edge turbulence with local dimensionless plasma parameters, e.g. collisionality, beta, or normalized gyroradius. However, it is often difficult to take into account the possible influence of other factors such as edge magnetic topology, the geometry of the limiters and/or divertor plates, the presence of neutrals, impurities, or radiation [140], the level of coherent MHD activity, or edge electric fields and rotation. Thus a definitive scaling of edge turbulence has not yet been achieved.

6) Intermittency and Coherent Structures

Large but intermittent transient events are often seen in the time series of edge turbulence signals, particularly in the SOL. The average level of intermittency can be characterized by the shape of the probability distribution function (PDF) of the amplitude distribution, as illustrated in Fig. 4 from TEXTOR tokamak [75]. Qualitatively similar intermittency in the edge density, potential and transport flux have been seen on many toroidal fusion devices, e.g. the ADITYA tokamak [141], T-10 [142], CASTOR [143], DIII-D [137], MAST[144], Tore-Supra [144], W7-AS [65], the TJ-K torsatron [92], and RFX [91,145]. Similar intermittency has been seen in linear devices (see Sec. 6.1).

Generally the skewness is positive in the SOL (i.e. dominated by large amplitude events), but is sometime negative inside the separatrix or limiter radius (i.e. with density 'holes'), e.g. in DIII-D [62] and the linear machine LAPD [146]. About half of the turbulent transport through the SOL has been attributed to these intermittent events, e.g. in DIII-D [62] and RFX [119], which makes them important for understanding the plasma-wall interaction.

The intermittency seen in time series data is most likely associated with coherent structures, which are relatively long-lived, self-organized (but not periodic) 'objects' which move within the turbulence. Coherent structures have been seen in neutral fluids [147], but are difficult to identify since their structure and motion are not necessarily reproducible. Coherent structures in edge turbulence are often called 'intermittent objects' or 'blobs', and are usually measured as the 2-D structure perpendicular to B of the 3-D

filaments. Attempts have been made to characterize edge coherent structures using 2-D space vs. time measurements [46,86,143,148], conditional sampling [62,85,137], and wavelet analysis [149]. The parallel structure of blobs has not yet been measured, but appears to be similar to that of the broadband turbulence.

The interplay between intermittent transport events and sheared flows is an active area of research (see Sec. 5.8). The probability distribution functions become more Gaussian in the presence of perpendicular sheared flow, and fluctuation signals show a bursty character with spikes that are asymmetric in time. This time asymmetry of fluctuation events is minimum close to the shear layer [57]. These characteristics have been observed both in fusion and low temperature plasmas.

7) L-mode vs. H-mode

In tokamaks and stellarators there can be a spontaneous transition from low (L-mode) to high (H-mode) confinement usually associated with the formation of an edge transport barrier. The observed changes in edge turbulence from L-mode to H-mode are correlated with changes in edge flows (see Sec. 5.8), and at least a transient reduction in turbulent transport (see Sec. 5.9). Similar transitions can be externally created by biasing electrodes in the edge (see Sec. 5.10).

Comparisons of edge turbulence measurements in L-mode vs. H-mode plasmas have been made with all types of edge turbulence diagnostics.

Heavy ion beam probe measurements showed a sudden decrease in the edge potential just inside the separatrix at the L-H transition, followed by at least a transient reduction in the edge density fluctuation level [150]. Edge density fluctuation levels later in the H-mode phase sometimes recover to their L-mode levels [32,151-153], possibly due to the increased edge pressure gradient in H-mode. A reduction of T_e fluctuations was associated with the shear flow in biased H-modes in TEXTOR [99].

Turbulence levels in the SOL seem to be only slightly reduced in H-mode, as illustrated in Fig. 1 [110,131,153]. Interestingly, edge turbulence measured using scattering in W7-AS was *higher* in the high density H-mode than in the normal confinement mode [27].

There is less evidence about the changes in turbulence size scale at the L-H transition. An increase in the poloidal correlation length from L-mode to H-mode was observed on PBX-M tokamak [154], but no significant changes in the radial correlation length were observed on ASDEX [155], NSTX [117] or Alcator C-Mod [153].

Changes were seen at the L-H transition in DIII-D in the intermittency [137], bispectral coupling [156], and nonlinear dynamics [157]. Langmuir probe measurements have also seen a change in the phase and correlation coefficient between the density and potential fluctuations which enters into the turbulent transport rate [158,159]. A difference between the long-time period correlations in L-mode and H-mode was seen in MAST [71]. Other measurements of the L-H transition are mentioned in the next 3 sections.

8) Edge flows

The relationship between edge flows and the edge turbulence is an interesting and complicated subject. Most of this work has focused on the 'shear layer' formed by the DC radial electric field just inside the limiter or magnetic separatrix [e.g. 160-162]. This shear layer can in theory cause a radial decorrelation and/or 'suppression' of edge turbulence and turbulent transport.

In TEXT tokamak there was some reduction in the turbulence observed within the shear layer in Ohmic (L-mode) plasmas [163]. In the TJ-II stellarator [161] and in JET [164] there appeared to be a marginal stability between shear flow and edge turbulence levels. Interestingly, in DIII-D there was a better correlation between the L-H transition and the edge turbulence phase velocity rather than the ExB flow velocity [165].

Some insight into the possible origin of the edge shear flows has been obtained by measuring the Reynold's stress R, which estimates the rate of momentum transfer between the mean flow and the turbulence; e.g. for tokamaks and stellarators:

$$R = - \langle \delta v_{rad} \, \delta v_{pol} \rangle \qquad [3]$$

(for RFPs, poloidal is replaced by toroidal). A recent result of this measurement using 4 Langmuir probes in JET is shown in Fig. 5(a), where the turbulence mean energy production term is compared with the poloidal mean flow. This indicates (surprisingly) that the energy transfer is from the

mean flow to the turbulence within the region of the shear layer ($r-r_{sep}$ = -20 to -10 mm) [166]. Reynold's stress measurements have also been made on several devices, e.g. the TJ-II stellarator [167], the ISTTOK tokamak [168], the HT-6M [169] and HT-7 tokamaks [170]; and the H-1 heliac [171]. In the Extrap-T2R RFP experiment the driving role of electrostatic fluctuations was demonstrated by the spatial structure of Reynolds stress and by the time behaviour of the mean energy production term, which supports the existence of an energy exchange from small scales of turbulence to the larger scales of mean flow in the inner shear region [172], as shown in Fig. 5(b). The electrostatic fluctuations are found to counterbalance anomalous viscous damping [173].

Measurements on the H-1 heliac have suggested that edge zonal flows can trigger an H-mode like transition [174]. Evaluation of the bicoherence has suggested poloidal flow generation preceding the H-mode transition in DIII-D [60] but not in NSTX [61].

Low frequency zonal flows in the edge density fluctuations have been directly measured recently on several devices. Most have been of the coherent geodesic acoustic mode (GAM), e.g. in DIII-D [45,175] and ASDEX-Upgrade [36], but some observations have also been made of broadband lower frequency flows, e.g. in the CHS stellarator [54] and JFT-2M tokamak [176].

Recently, radial profiles of the parallel-radial Reynolds stress component have been measured in the plasma boundary region of the TJ-II stellarator [177]. Experimental results show the existence of significant

parallel turbulent forces at plasma densities above the threshold value to trigger perpendicular ExB sheared flows. These results suggest parallel turbulent force is also an important ingredient to explain flow momentum re-distribution in the boundary of fusion plasmas (i.e. shear flow physics requires a 3-D description). Due to the 3-D nature of the shear flow physics in fusion plasmas, several components of the production, including radial-parallel and radial-perpendicular components of Reynolds stress, term should considered [178]. In addition, turbulent events (blobs) can provide an additional mechanism for flow generation via Reynolds stress (e.g. eddy tilting). Quantifying the importance of such mechanisms is an active area of research [e.g. 86].

9) Turbulent transport

The radial particle transport due to edge turbulence is usually evaluated from edge turbulence measurements by assuming the local radial drift velocity is given by $v_r = E_{pol}/B$, i.e.:

$$\Gamma_n^{rad} = \langle \delta n \, \delta v_r \rangle = \langle \delta n \, \delta E_{pol} \rangle / B \qquad [4]$$

(where poloidal is replaced by toroidal for an RFP). Thus the transport flux depends on the correlation coefficient and phase angle between the measured δn and δE_{pol}, and so can not be estimated from δn alone. The magnetic fluctuation contribution to this particle flux is generally negligible [2-5].

This ExB particle flux has been measured near the outer midplane of many fusion devices using three nearby Langmuir probes, resulting in a large outward radial transport roughly consistent with the total particle loss rate across the last closed flux [e.g. 2-5; 179]. However, the radial profile of the turbulence-induced flux of Eq. (3) is generally not constant across the edge, suggesting other particle balance effects are also present such as poloidal asymmetry, local ionization, parallel loss to the wall, large scale convective cells [180] and/or neoclassical transport.

The PDF of the radial velocity in Eq. 1 has also been shown to have strong non-Gaussian features in the SOL of JET [164]. It was shown that about half of the SOL radial transport is due to convective radial motion of the intermittent coherent structures in DIII-D [62,110] and in RFX [119]. Similar results have been obtained on Heliotron J [181] and Alcator C-Mod [182].

Thus the radial particle transport in the SOL has a significant "ballistic" or "convective" flow component and is not simply a diffusive process, as previously assumed [7]. This convective flux can cause large radial transport in regions with a shallow gradient, and so can deposit particles and energy in unexpected places.

The radial electron heat transport can be due to either to electrostatic or magnetic fluctuations, e.g. as in [4] (Table IV):

$$Q_e^{rad} = n\langle \delta v_r \, \delta T_e \rangle + T_e \langle \delta v_r \, \delta n \rangle + \langle Q_{ll} \, \delta B_r \rangle / B \qquad [5]$$

where B_r is the turbulent radial magnetic field fluctuation level. The second (heat conduction) term was measured to be significant in TEXTOR [183]. The last (magnetic fluctuation) term has been measured in the edge of a few devices, where it was small compared with first term (i.e. the particle flux) [108,184,185]. The radial ion heat transport due to edge turbulence has not yet be measured.

To clarify the mechanisms that are at work, it is important to understand the possible link between the radial velocity and other properties of the transport events, and to compare the radial transit time of the blob to the plasma wall with the characteristic time of transport to the divertor plates along the magnetic field. The order of magnitude of the measured radial blob propagation velocity suggests that a competition between both parallel and radial transport is needed to explain particle losses in the SOL region of fusion plasmas (i.e. to predict the particle and energy fluxes onto the divertor plates in ITER).

10) Turbulence control

It would be useful to be able to directly control edge turbulence since the edge transport can not yet be predicted for future burning plasma devices. For example, it would be to useful to learn how to increase the SOL thickness in order to spread the heat over a wider region at the divertor plates, while at the same time avoiding damage to first wall structures near the outer midplane.

Edge turbulent transport has been changed in many experiments by inserting biased electrodes into the plasma, as reviewed recently [186]. These experiments have found a correlation between edge shear flow and turbulent transport reduction, e.g. in the TEXTOR tokamak [183], in the KT-5C tokamak [187] and RFX [188]. Similar experiments have been done using the less intrusive biasing of limiter and/or divertor plates, e.g. on the ISTTOK tokamak [189]. Floating potential fluctuations in the SOL were reduced by a positive limiter bias and increased by a negative limiter bias on the STOR-M tokamak [190], and large fluctuation events were reduced by a negatively biased emissive electrode in ISTTOK [191]. Biasing experiments in the TJ-II stellarator showed improved confinement regimes similar to tokamaks, e.g. [192].

Experiments in Tore-Supra have shown a decrease in turbulence at large size scales and low frequencies with an ergodic divertor, at least a low density [193]. The effect of a rotating helical magnetic field on the fractal structure of edge turbulence was studied on the HYBTOK-II tokamak [68]. Edge turbulence has been changed by the introduction of RF waves into the edge plasma; for example, by Alfven waves in the TCABR tokamak [194], and by lower hybrid waves in the HT-7 tokamak [195]. Plasma wall conditions also seemed to influence the edge turbulence in HT-7 [196].

Active control of edge turbulence using AC biased probes was first attempted on TEXT using both periodic forcing and feedback [197]. More recently periodic driving experiments were done on W7-AS [198], where it was concluded that a subdivided array of actively biased divertor targets might be able to control edge turbulence in fusion devices. Mode selective

control of drift wave turbulence was also investigated experimentally and theoretically in a linear device MIRABELLE [199].

6. Discussion

This section discusses the results of Sec. 5 in relation to non-fusion magnetized plasmas (Sec. 6.1) and to edge turbulence theory (Sec. 6.2). It also presents some directions for further research (Sec. 6.3) and a summary and conclusion (Sec. 6.4).

6.1 Comparison with non-fusion devices

As discussed in Sec. 5.1-5.3, edge density turbulence has similar characteristics in all toroidal fusion devices, e.g. tokamaks, stellarators, and RFPs [e.g. 4,114,200]. Qualitatively similar turbulence is also seen in the interior of simple magnetized toroidal plasmas (with no plasma current); for example in Blaamann [201], TEDDI [202], BETA [203], and TORPEX [204]. This shows that closed magnetic surfaces are not essential for the formation of edge turbulence, which is not surprising given the similarity of edge turbulence across the last closed flux surface in fusion devices.

Plasma intermittency measured in linear devices sometimes has properties similar to those in toroidal fusion devices, for example, in a Q-machine [205], LAPD [146]. PISCES [206] and Mistral [207]. Instabilities in some linear devices tend to be dominated by a few well defined mode structures rather than broadband turbulence, e.g. in VINETA [208], and the

Columbia Linear Machine [209]. Thus the transition from discrete modes to turbulence can be studied, e.g. in KIWI [202] and CSDX [210,211] and in a low beta plasma column [212].

6.2 Comparisons with theory

Many experimental papers on edge turbulence have attempted to compare their results with a theory or numerical simulation of edge turbulence. Until recently these comparisons were done using linear theory or simplified nonlinear models [1-6]. More recently they have been done using generalized nonlinear dynamics models or direct numerical simulation [8]. Some of the more recent comparisons between experiment and theory in edge turbulence will be summarized here.

Some insight into edge turbulence physics can be gained by searching for statistical patterns in the data and comparing them to general models of nonlinear dynamics. Evidence for self-similarity and long-range correlations in edge turbulence was found by evaluating the Hurst parameter for various devices [71,213]. Since then there have been several analyses of the self-similarity, self-organized criticality (SOC), and 'universality' of the statistical properties of edge turbulence using data from various stellarators, tokamaks, and linear devices [65,72,144], e.g. W7-AS, TJ-1U and JET, Tore-Supra, MAST, Alcator C-Mod, PISCES, W7-AS, and TJ-II. Self-similarity of density turbulence in the far-SOL was also observed in the TCV tokamak [214], and in RFX-mod [215]. Time-correlated groups of bursts were observed in the SOL of CASTOR and identified with radial 'fingers' in an interchange model [216]. Evidence for SOC-like behaviour

in DIII-D was described in [217]. A search for SOC in RFX showed results inconsistent with this model [73], although a modified SOC model was more consistent with the data [218].

Another approach to experiment-theory comparisons of edge turbulence is to use analytic models to study the scaling with specific dimensionless parameters. For example, scalings of edge turbulence with drift wave theory parameters were done in TEXT [134], and the scaling of turbulence with the velocity shear induced by edge biasing was compared with various analytic theories in TEXTOR [219]. The scaling of the turbulence size scale with ρ_s was studied in DIII-D [120] and TJ-K [135], and a ccomparison of edge radial correlation lengths just inside the separatrix in DIII-D with analytic models was done in [220]. Identification of vortex-like coherent structures in edge turbulence was made in ADITYA [221] and RFX [119].

Direct comparisons of analytic 'blob' models with experimental results are beginning to be made, e.g. on NSTX [222]. From the theoretical point of view, some models conclude that the radial speed increases as the squared root of the blob size [223] predict a radial blob velocity inversely proportional to the blob size. In the first case, the larger the size, the more important the radial transport, implying an increase of plasma-wall interaction in large fusion devices (which may have an impact on the final choice of plasma wall protection in ITER).

Direct comparisons between edge turbulence measurements and numerical simulations are difficult and need to be done on a case-by-case basis. One example is illustrated in Fig. 6 for the plasma in the SOL of the

TCV tokamak [224]. This comparison show good agreement between probe measurements and the 2-D nonlinear interchange code ESEL, but some details such as the 3-D magnetic geometry have not yet been included in the model.

Comparisons of the DIII-D fluctuation measurements with theory (mainly for the core plasma) were reviewed in [225]. Measurements of the k_{pol} spectrum of edge turbulence in Alcator C-Mod were in fairly good agreement with a 3-D nonlinear fluid turbulence code NLET, at least in the SOL [115]. Measurements of the frequency spectrum and amplitude of the L-mode edge turbulence in ASDEX-Upgrade were in tentative agreement with the DALFTI turbulence code just inside the separatrix [39]. The measured frequency spectrum in the TJ-K torsatron was similar to the spectrum calculated for the same dimensionless parameters by the DALF3 code [226,227]. Initial comparisons of the simulation results from the BOUT edge turbulence code with edge turbulence measured in DIII-D were described in [131,137,228]. A comparison of SOL profiles (but not turbulence) with the fluid turbulence model 'phase space' parameters was done for Alcator C-Mod [139].

In some sense the similarity of edge turbulence across many devices with different magnetic geometry and plasma parameters makes it more difficult to isolate the physical 'drive' and 'damping' responsible for the turbulence in specific devices. However, such 'universality' seems to be real and qualitatively similar to normal fluid turbulence.

6.3 Directions for Further Research

Despite much good effort, there is still considerable uncertainty about the dimensionless scalings (Sec. 5.5), the causes of intermittency (Sec. 5.6), and the L-H transition (Sec 5.7), the relationship of flows and turbulence (Sec. 5.8), and the transport processes which determine the heat and particle loads on the first wall (Sec. 5.9). Many of these phenomena seem to be interrelated; for example, the study of the properties of large intermittent events (blobs) has recently changed the standard (diffusive) picture of turbulent transport in the SOL, and the possible coupling between intermittency and plasma flows is an active area of research. Improved connections between theory and experiment will be necessary to untangle and understand these complex interactions.

Significant progress on the characterization of edge turbulence could be made using existing diagnostics on present devices. The poloidal distribution of the turbulence levels in diverted tokamaks can be measured to clarify the causes of asymmetry. The parallel wavelength could be more accurately measured to determine whether the turbulence is drift-like or flute-like in various regimes and devices. The scaling of the turbulence levels with dimensionless plasma parameters should be revisited, keeping in mind the possible influence of neutral and/or atomic physics.

There is also room for new diagnostics of edge turbulence. Non-perturbing optical measurements of turbulent velocity fluctuations might be made using interference filters [229]. Measurements of fluctuations in the ion distribution function might be made using laser-induced fluorescence to

evaluate kinetic effects on edge turbulence [230]. The speed of IR cameras might be further increased to measure the heating due intermittent structures on the first wall [231]. It would be highly desirable to measure edge magnetic turbulence without probes, but no good technique is available.

Despite the progress of recent experiment-theory comparisons, it is still not possible to predict edge transport from "first-principles", e.g. for the SOL thickness in ITER. Thus it would be useful and interesting to develop methods to actively control edge turbulence. Some ideas have already been tested, as discussed in Sec. 5.10. Untested ideas include the creation of convective cells by limiter biasing to increase the SOL width [232], and the creation of a transport barrier to reduce the SOL width [233]. It is also possible that edge turbulence could be controlled by creative applications of RF waves or particle fueling.

6.4 Summary and Conclusion

This paper has reviewed measurements of edge turbulence in toroidal fusion devices in terms of the fluctuation levels, frequency spectra, size scales, poloidal distributions, parameter scalings, intermittency, L-H transitions, edge flows, and transport. To a first approximation, the nature of edge turbulence is qualitatively similar in all regimes and devices, although there are also significant variations within any single device.

Some noteworthy recent advances include 2-D imaging diagnostics, identification of intermittency as a significant SOL transport mechanism, and evaluation of the coupling between edge turbulence and flows. There

have also been significant improvements in the analysis of the non-linear dynamics, e.g. using the Reynold's stress and bicoherence techniques.

However, many physics issues still remain unresolved from the experimental perspective. Recent advances in the comparison of turbulence measurements with numerical simulations may help to resolve these issues in the near future. The need for improved predictability and/or active control of edge turbulence is also becoming increasingly apparent (see Sec. 5.10), therefore the invention and testing of new ideas in these areas is a timely challenge.

Acknowledgments: We thank all the people whose research is summarized in this review and apologize for the omissions. This work was supported by DOE contract #DE-AC02-76CHO3073.

References

[1] Surko CM et al, Science 221 (1983) 817 ;

[2] Liewer, PC, Nucl. Fusion **25** (1985) 1281

[3] Wootton, AJ et al, Phys. Fluids **B2** (1990) 2879

[4] Carreras, BA, IEEE Trans. Plasma Sci. **25** (1997) 1281

[5] Endler, M, J. Nucl. Mater. **266-269** (1999) 84

[6] Horton W, Rev. Mod. Phys. 71 (1999) 735

[7] Stangeby P, The Plasma Boundary of Magnetic Fusion Devices, IOP, Bristol (2000)

[8] Carreras, BA, J. Nucl. Mater. **337-339** (2005) 315

[9] Bohm D et al, The Characteristics of Electrical Discharges in Magnetic Fields, ed. A. Guthrie and R.K. Wakerling, McGraw-Hill (1949)

[10] Nedospasov, AV, J. Nucl. Mat. **196-198** (1992) 90

[11] Chen, FF, Phys. Rev. Lett. 15, (1965) 381

[12] Young KM, Phys. Fluids **10** (1967) 213

[13] Robinson DC and Rusbridge MG, Phys. Fluids **14** (1971) 2449

[14] Powers E, Nucl. Fusion 14 (1974) 749

[15] Davidson PA, Turbulence, Oxford University Press, 2004

[16] Bretz N, Rev. Sci. Inst. **68** (1997) 2927

[17] Hartfuss HJ et al, Plasma Phys. Cont. Fusion 39 (1997) 1693

[18] Gentle KW, Rev. Modern Phys. **67** (1995) 809

[19] Hutchinson IH, Principles of Plasma Diagnostics, 2nd Edition, Cambridge University Press (2002)

[20] Donne AJH, Fusion Science and Technology **45** (2004) 399

[21] Demidov VI et al K, Rev. Sci. Inst. **73** (2002) 3409

[22] LaBombard B, Phys. Plasmas **9** (2002) 1300

[23] Calderon E et al, Rev. Sci. Inst. **75** (2004) 4293

[24] Mazzucato E, Phys. Rev. Lett. **36** (1976), 792

[25] Surko CM et al, Phys. Rev. Lett. **37** (1976) 174

[26] Brower DL et al, Nucl. Fusion **27** (1987) 2055

[27] Basse NJ et al, Nucl. Fusion 43 (2003) 40

[28] Watterson RL et al, Phys. Fluids **28** (1985) 2857

[29] Saffman M et al, Rev. Sci. Inst. 72 (2001) 2579

[30] Porkolab M et al, IEEE Trans. Plasmas Sci. 34 (2006) 229

[31] Nazikian R et al, Phys. Plasmas **8** (2001),1840

[32] Wang G et al. Plasma Phys. Cont. Fusion **46** (2004) A363

[33] Rhodes TL et al, Plasma Phys. Cont. Fusion 40 (1998) 493

[34] Gilmore M et al, Rev. Sci. Inst 72 (2001) 293

[35] Kramer GJ et al, Rev. Sci. Inst. **74** (2003), 1421

[36] Conway GD et al., Plasma Phys. Cont. Fusion **47** (2005) 1165

[37] Heuraux S et al., Rev. Sci. Inst. **74** (2003), 1501

[38] Bruskin LG et al., Plasma Phys. Cont. Fusion 47 (2005) 1379

[39] Conway GD et al, Plasma Phys. Cont. Fusion **44** (2002) 451

[40] Goodall DHJ, J. Nucl. Mat. 111/112 (1982) 11

[41] Endler M et al, Nucl. Fusion 35 (1995) 1307

[42] Huber A et al, J. Nucl. Mat. 266-269 (1999)

[43] Carraro L et al., Rev. Sci. Inst. **72** (2001) 967

[44] Maqueda RJ *et al*, Rev. Sci. Inst. **74**, (2003) 931

[45] McKee GR *et al*, Phys. Plasmas 10, 1712 (2003)

[46] Zweben SJ *et al*, Nucl. Fus. **44**, 134 (2004) 134

[47] Bruchhausen M et al, Plasma Phys. Cont. Fus. 46 (2004) 489

[48] Cavazzana R et al, Rev. Sci. Inst. 75 (2004) 4152

[49] Zoletnik S et al., Rev. Sci. Inst. **76** (2005), 2020

[50] Zweben S et al, Nucl. Fusion 23 (1983) 825

[51] Ritz CP et al., Phys. Rev. Lett. 62 (1989) 1844

[52] Nakano H et al., Rev. Sci. Inst. **75** (2003) 3505

[53] Schoch PM et al, Rev. Sci. Inst. 74 (2003) 1843

[54] Fujisawa A, et al, Phys. Rev. Lett. **93**, 165002 (2004)

[55] Hamada Y et al, Phys. Rev. Lett. **96** (2006) 115003

[56] Beall JM et al, J. App. Phys. 53 (1982) 3933

[57] Sánchez E et al, Plasma Phys. 7 (2000) 1408

[58] van Milligen BP et al, Phys. Plasmas 2 (1995) 3017

[59] Kim JS et al, Phys. Rev. Lett. 79 (1997)

[60] Tynan GR et al, Phys. Plasmas 8 (2001) 2691

[61] White AE et al, Phys. Plasmas 13 (2006) 072301

[62] Boedo JA et al, Phys. Plasmas 8, (2001) 4826

[63] Antoni V et al, Europhys. Lett. 54 (2001) 511

[64] Baptista MS et al, Phys. Plasmas 10 (2003) 1283

[65] van Milligen BP et al, Phys. Plasmas 12 (2005) 052507

[66] Farge M et al, Phys. Plasmas 13 (2006) 042304

[67] Komori A et al., Phys. Rev. Lett. 73, (1994) 660

[68] Budaev V et al., Nucl. Fusion 44 (2004), S108

[69] Carreras B et al, Phys. Plasmas 5 (1998) 3632

[70] Jha R et al, Phys. Plasmas 10 (2003) 699

[71] Dudson BD et al, Plasma. Phys. Cont. Fusion 47 (2005) 885

[72] Carreras BA et al., Phys. Plasmas 6 (1999) 1885

[73] Spada E et al, Phys. Rev. 86 (2001) 3032 ;

[74] Sanchez R et al, Phys. Rev. Lett. 90 (2003) 185005

[75] Xu YH et al, Plasma Phys. Cont. Fusion 47 (2005) 1841

[76] Bleuel J et al, New J. Physics 4, (2002) 38.1

[77] Bruchhausen M et al, Plasma Phys. Cont. Fus. 46 (2004) 489

[78] Block D et al, Phys. Scr. T122 (2006) 25

[79] Grulke O et al, Plasma Phys. Cont. Fusion 43 (2001) 525

[80] Rudakov DL et al, Plasma Phys. Cont. Fusion 44 (2002) 717

[81] McKee GR et al, Rev. Sci. Inst. 74 (2003) 2014

[82] Jakubowski M et al, Rev. Sci. Inst. 72 (2001) 996

[83] Holland C et al, Rev. Sci. Inst. 75 (2006) 4278

[84] Terry JL et al, J. Nucl. Mat. 337-339 (2005) 322

[85] Grulke O et al, Phys. Plasmas 13 (2006) 102306

[86] Alonso JA et al, Fusion Science and Tech. 50 (2006) 310

[87] Munsat T, to be published in Rev. Sci. Inst (2006)

[88] Zabusky NJ, Ann. Rev. Fluid Mech. 495 (1999) 536

[89] Farge M, Annu. Rev. Fluid. Mech. 24 (1992) 395

[90] Onorato M et al., Phys. Rev. E 61 (2000) 1447

[91] Carbone V et al., Phys. Plasmas 7 (2000) 445

[92] Mahdizadeh N et al., Phys. Plasma 11(2004) 3932

[93] Frisch U in Turbulence: the legacy of A. N. Kolmogorov, ed. Cambridge University Press 1995

[94] Moyer RA et al, J. Nucl. Mat. 266 (1997) 633

[95] Durst RD et al, Phys. Rev. Lett. 71 (1993) 3135

[96] Hanson GR et al, Nucl. Fusion 32 (1992) 1593

[97] Antoni V et al, Phys. Rev. Lett. 80 (1998) 4185

[98] Martines E et al, Nucl. Fusion 39 (1999) 581

[99] Boedo JA et al, Phys. Rev. Lett. 84 (2000) 2630

[100] Meier M.A. et al, Phys. Rev. Lett. 87 (2001) 085003

[101] Kumar R et al, Nucl. Fusion 43 (2003) 622

[102] Pericoli-Ridolfini V et al, Nucl. Fusion 38 (1998) 1745

[103] Silva C et al, Rev. Sci. Inst. 75 (2004) 4314

[104] Zweben SJ et al, Nucl. Fusion 21 (1981) 193

[105] Graessle DE et al, Phys. Fluids B 3 (1991) 2626

[106] Stockel J et al, Plasma Phys. Cont. Fusion 41 (1999) A577

[107] Sarff JS et al, Phys. Fluids B 5 (1993) 2540

[108] Serianni G et al, Plasma Phys. Cont. Fusion 43 (2001) 919

[109] LaBombard B et al, Phys. Plasmas 8 (2001) 2107

[110] Rudakov DL et al, Nucl. Fusion 45 (2005) 1589

[111] Pedrosa MA et al, Phys. Rev. Lett. 82 (1999) 3621

[112] Bol, K, Phys. Fluids 7 (1964) 1855

[113] Hidalgo C et al, Plasma Phys. Cont. Fusion 47 (2001) A313

[114] Antoni V, Plasma Phys. Cont. Fusion 39 (1997) B223

[115] Terry et al, Phys. Plasmas **10**, 1739 (2003)

[116] McKee et al, Rev. Sci. Inst. 75 (2004) 3490

[117] Zweben SJ et al, Phys. Plasmas **13** (2006) 056114

[118] Huber A et al, Plasma Phys. Cont. Fusion 47 (2005) 409

[119] Spolaore M et al., Phys. Rev. Lett. 93 (2004) 215003

[120] McKee GR et al, Nucl. Fusion 41 (2001) 1235

[121] Bengtson RD et al, Contrib. Plasma Phys. 38 (1998) 104

[122] Thomsen H et al, Phys. Plasmas 9 (2002) 1233

[123] Zweben SJ et al, Phys. Fluids B1 (1989) 2058

[124] Tynan G et al, Plasma Phys. Cont. Fusion **38**, (1996) 1301

[125] Devynck P et al, Plasma Phys. Cont. Fusion **47** (2005) 269

[126] Vershkov VA et al, J. Nucl. Mat. 241-243 (1997) 873

[127] Kirnev GS et al, Nucl. Fusion 45 (2005) 459

[128] Fenzi C et al, Nucl. Fusion 40 (2000) 1621

[129] Tanaka K et al, Nucl. Fusion 46 (2006) 110

[130] Smick N et al, J. Nucl. Mat. 337-339 (2005) 281

[131] Moyer RA et al., J. Nucl. Mat. 266 (1999) 1145

[132] Antar, GY et al, Phys. Plasmas **12** (2005) 032506

[133] Endler M, Plasma Phys. Cont. Fusion 41 (1999) 1431

[134] Rhodes TL et al, Nucl. Fusion 33 (1993) 1147

[135] Ramisch M et al, Phys. Plasmas 12 (2005) 032504

[136] Zweben, SJ et al, Nucl. Fusion 23 (1983) 1625

[137] Boedo JA et al, Phys. Plasmas 10 (2003) 1670

[138] Greenwald M, Plasma Phys. Cont. Fusion 44 (2002) 27

[139] LaBombard B et al, Nucl. Fusion 45 (2005) 1658

[140] Pedrosa MA et al, Phys. Plasmas 2 (1995) 2618

[141] Jha R et al, Phys. Rev. Lett. (1992) 1375

[142] Kirnev GS et al, J. Nucl. Mat. 337 (2005) 352

[143] Martines E et al, Plasma Phys. Cont. Fusion 44 (2002) 351

[144] Antar GY et al, Phys. Plasmas 10 (2003) 419

[145] Sattin F et al., Phys Plasma 11 (2004) 5032

[146] Carter TA, Phys. Plasmas (2006) 010701

[147] Schoppa W and Hussain F, J. Fluid Mech 453 (2002) 57

[148] Zweben SJ, Phys. Fluids 28 (1985) 974

[149] Dong L et al, Phys. Rev. E 57 (1998) 5929

[150] Ida K et al, Fusion Science and Technology 49 (2006) 122

[151] Ido T et al, Phys. Rev. Lett. (2002) 055006

[152] Moyer RA, Plasma Phys. Cont. Fusion 41 (1999) 243

[153] Terry JL et al, Nucl. Fusion 45 (2005) 1312

[154] Tynan GR et al, Phys. Plasmas 1 (1994) 3301

[155] Kurzan B et al, Plasma Phys. Cont. Fusion 42 (2000) 237

[156] Moyer RA et al, Phys. Rev. Lett. 87 (2001) 135001

[157] Moyer RA et al, Plasma Phys. Cont. Fusion 38 (1996) 1273
[158] Tynan G et al, Plasma Phys. Cont. Fusion 36 (1994) A285
[159] Moyer RA et al, Phys. Plasmas 2 (1995) 2397
[160] Ritz CP et al, Phys. Fluids 27 (1984) 2956
[161] Pedrosa MA et al, Plasma Phys. Cont. Fusion 47 (2005) 777
[162] Antoni V et al, Plasma Phys. Cont. Fusion 47 (2005) B13
[163] Ritz CP et al, Phys. Rev. Lett 65 (1990) 2543
[164] Goncalves B et al, J. Nucl. Mat. 337 (2005) 376
[165] Fenzi C et al, Phys. Plasmas 12 (2005) 062307
[166] Sanchez E et al, J. Nucl. Mat. 337 (2005) 296
[167] Hidalgo C et al, Plasma Phys. Cont. Fusion 42 (2000) A153
[168] Hidalgo C et al, Phys. Rev. Lett. 83 (1999) 2003
[169] Xu YH et al, Phys. Rev. Lett. 84 (2000) 3867
[170] Xu GS et al, Phys. Rev. Lett. 91 (2003) 125001
[171] Xia H et al, Phys. Plasmas 11 (2004) 561
[172] Vianello N et al., Plasma Phys. Control. Fusion 48 (2006) S193
[173] Vianello N et al., Phys. Rev. Lett. 94 (2005) 135001
[174] Punzmann H et al, Phys. Rev. Lett. 93 (2004) 125003
[175] McKee GR et al, Plasma Phys. Cont. Fusion 45 (2003) A477
[176] Nagashima Y et al, Phys. Rev. Lett. 95 (2005) 095002
[177] Goncalves B et al, Phys. Rev. Lett. 96 (2006) 145001
[178] Hidalgo C et al, Plasma Phys. Contr. Fusion 48 (2006) S169
[179] Rempel TF et al, Phys. Fluids B 4 (1992) 2136
[180] Tynan GR et al, Phys. Rev. Lett. 68 (1999) 3032
[181] Mizuuchi T et al, J. Nucl. Mat. 337 (2005) 332
[182] Carreras BA et al, Phys. Plasmas 8 (2001) 3702
[183] Boedo JA et al, Nucl. Fusion 40 (2000) 1397

[184] Fiksel G et al, Phys. Rev. Lett. 72 (1994) 1028
[185] Fiksel G, Phys. Rev. Lett. 75 (1995) 3866
[186] Van Oost G et al, Plasma Phys. Cont. Fusion 45 (2003) 621
[187] Wang C et al, IEEE Trans. Plasma Sci. 30 (2002) 625
[188] Antoni V et al, Plasma Phys. Cont. Fusion 42 (2000) 83
[189] Silva C et al, Plasma Phys. Cont. Fusion 46 (2004) 163
[190] Zhang W et al, Phys. Plasmas 1 (1994) 3646
[191] Silva C et al, Plasma Phys. Cont. Fusion 48 (2006) 727
[192] Hidalgo C et al., Plasma Phys. Cont. Fusion 46 (2004) 287
[193] Devynck P et al, Nucl. Fusion 42 (2002) 697
[194] Ferreira AA et al, Plasma Phys. Cont. Fusion 46 (2004) 669
[195] Ding BJ et al, Phys. Plasmas 11 (2004) 207
[196] Song H et al, Plasma Phys. Cont. Fusion 45 (2003) 1805
[197] Uckan T et al, Nucl. Fusion 35 (1995) 487
[198] Thomsen H et al, Plasma Phys. Cont. Fusion 47 (2005)0 1401
[199] Schroder C et al, Phys. Rev. Lett. 86 (2001) 5711
[200] Tsui HYW et al, Phys. Fluids B5 (1993) 2491
[201] Fredriksen A et al, Phys. Plasmas 10 (2003) 4335
[202] Grulke O et al, New Journal of Physics 4 (2002) 67.1
[203] Prasad G et al, Phys. Plasmas 1 (1994) 1832)
[204] Fasoli A et al, Phys. Plasmas 13 (2006) 055902
[205] Huld T et al, Phys. Fluids B3 (1991) 1609
[206] Antar GY, Phys. Plasmas 10 (2003) 3629
[207] Pierre T et al, Phys. Rev. Lett. 92 (2004) 065004
[208] Schroder C et al, Phys. Plasmas 12 (2005) 042103
[209] Chiu JS et al, Phys. Plasmas 7 (2000) 4492
[210] Burin MJ et al, Phys. Plasmas 12 (2005) 052320

[211] Holland C et al, Phys. Rev. Lett. 96 (2006) 195002
[212] Klinger T et al, Phys. Rev. Lett. 79 (1997) 3913
[213] Carreras B et al, Phys. Rev. Lett. 80 (1998) 4438
[214] Graves JP et al, Plasma Phys. Cont. Fusion 47 (2005) L1
[215] Sattin F et al., Plasma Phys. Control. Fusion 48 (2006) 1033
[216] Devynck P et al, Phys. Plasmas 12 (2005) 050702
[217] Rhodes TL et al, Phys. Lett. A 253 (1999) 181
[218] Sattin F et al, Phys. Rev. Lett. 96 (2006) 105005
[219] Boedo JA et al, Nucl. Fusion 42 (2002) 117
[220] Rhodes TL et al, Phys. Plasmas 9 (2002) 2141
[221] Joseph BK et al, Phys. Plasmas 4 (1997) 4292
[222] Myra JR et al, to be published in PoP
[223] Garcia OE et al, Phys. Of Plasmas 12 (2005) 090701
[224] Garcia OE et al, Plasma Phys. Cont. Fusion 48 (2006) L1
[225] Rhodes TL et al, Fusion Science and Tech. 48 (2005) 1042
[226] Stroth U et al, Phys. Plasmas 11 (2004) 2558
[227] Lechte C et al, New J. Physics 4 (2002) 34.1
[228] Xu XQ et al, New Journal of Physics 2 (2002) 53.1
[229] Paul SF et al, Rev. Sci. Inst. 75 (2004) 4077
[230] Diallo A et al, Phys. Plasmas 13 (2006) 055705
[231] Eich T et al, Plasma Phys. Cont. Fusion 47 (2005) 815
[232] Ryutov DD et al, Plasmas Phys. Cont. Fusion 43 (2001) 1399
[233] Figarella et al, J. Nucl. Mat. 337-339 (2005) 342

Figures Captions:

1) Profiles of edge plasma parameters and edge turbulence measured using a reciprocating Langmuir probe in D-IIID during Ohmic plasmas [131]. Qualitatively similar profiles are found in essentially all tokamaks and other toroidal fusion devices.

2) Comparison of the frequency spectrum of edge density turbulence from various stellarator and tokamak devices [111]. These spectra were all taken with Langmuir probes at the radius where the poloidal turbulence flow speed was near zero. The frequencies were rescaled by the factors shown the legends, and the amplitudes were rescaled to match each other. The edge turbulence spectra have a similar shape in most toroidal fusion devices.

3) Two dimensional structure of the edge turbulence perpendicular to the magnetic field in the Alcator C-Mod tokamak, as measured by the GPI diagnostic near the outer midplane separatrix [115]. The intensity of the D_α light emission in these 4 μsec exposures has been normalized to the time-averaged image. Qualitatively similar 2-D structure has been seen in many other toroidal fusion devices.

4) Evidence for intermittency in edge turbulence as measured by the non-Gaussian probability distribution functions (PDF) of edge density fluctuations in the TEXTOR tokamak [75]. These PDFs were measured by a Langmuir probe for the SOL at r/a=1.07 (left) and in the plasma edge at r/a=0.95 (right). The intermittency, skewness and kurtosis of these signals increase in the SOL. Similar intermittency is seen in the turbulence-induced

edge particle flux.

5) In (a), the poloidal velocity of edge turbulence and the turbulent Reynold's stress production, as measured using Langmuir probes in a limited Ohmic plasma in JET [166]. The positive direction of the Reynold's stress indicates energy transfer from the mean flow to the turbulence within the region of the shear layer ($r-r_{sep}$ = -20 to -10 mm). In (b) is the radial profile of the ExB toroidal drift in Extrap-T2R, along with the electrostatic and magnetic components of the Reynold's stress, in which the energy is transferred from the turbulence to the mean flow inside the last closed flux surface [172].

6) Comparison between edge turbulence measurements in the SOL of the TCV tokamak and numerical simulations from the ESEL code [224]. The horizontal coordinate is the 0 at the separatrix and 1 at the wall shadow. At the left is the radial profile of the autocorrelation time, and at the right is the conditionally-averaged time dependence of the density waveforms for intermittent bursts exceeding 2.5 times the standard deviation.

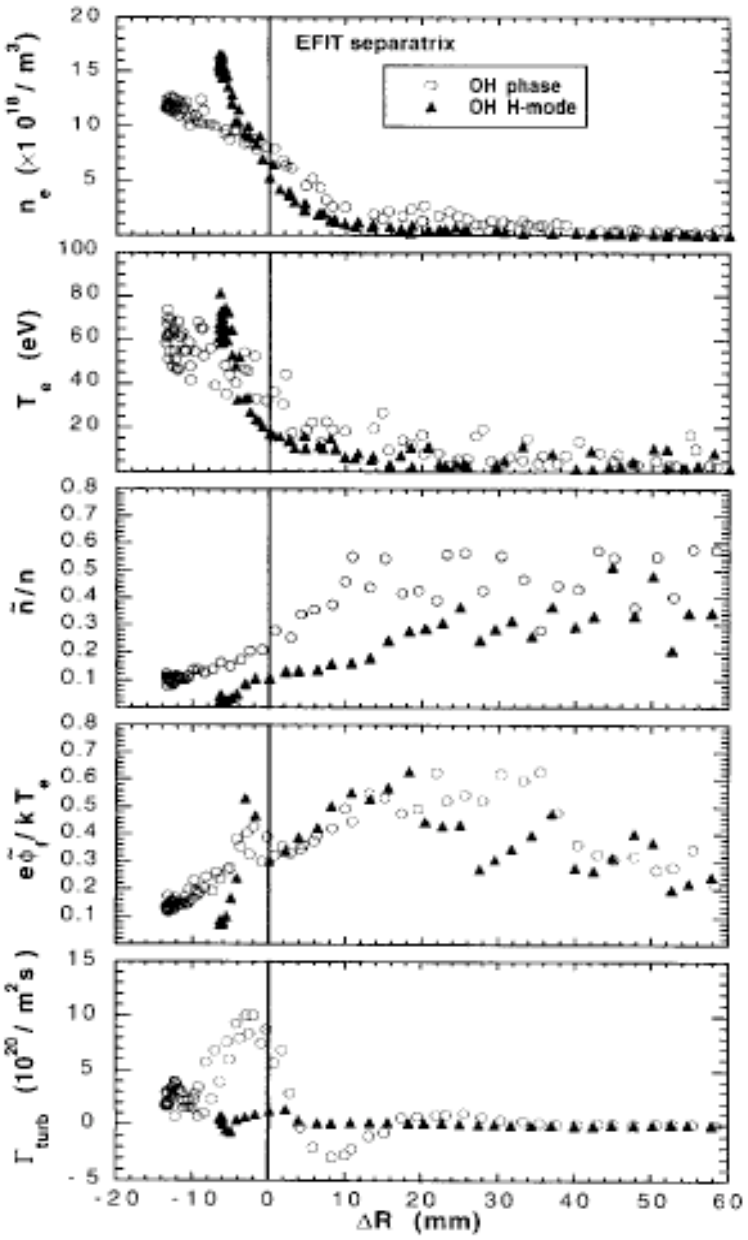
EFIT separatrix
OH phase
OH H-mode
n_e ($\times 10^{19}$ / m^3)
T_e (eV)
$\tilde{n}/n$
$e\tilde{\phi}/kT_e$
Γ_{turb} (10^{20} / m^{2}s)
ΔR (mm)

Fig. 1

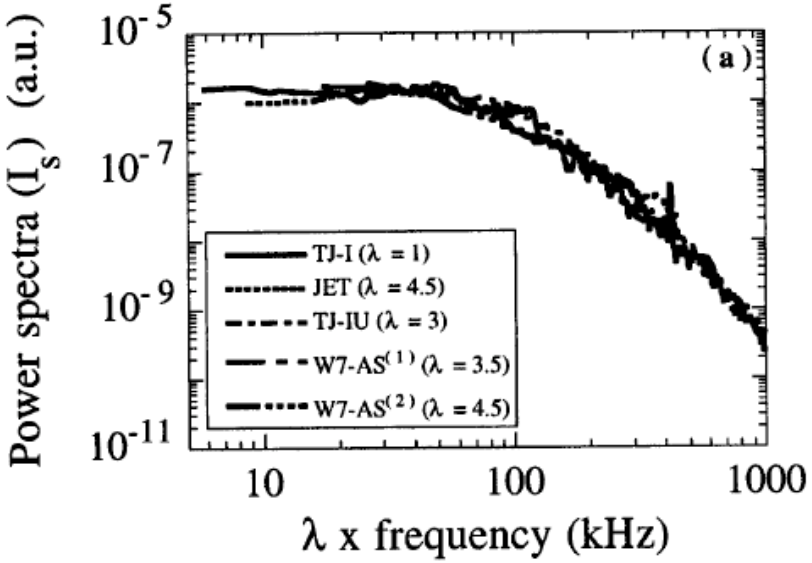
Power spectra (I_s) (a.u.)
10^{-5}
10^{-7}
10^{-9}
10^{-11}
(a)
TJ-I (λ = 1)
JET (λ = 4.5)
TJ-IU (λ = 3)
W7-AS(1) (λ = 3.5)
W7-AS(2) (λ = 4.5)
10
100
1000
λ x frequency (kHz)

Fig. 2

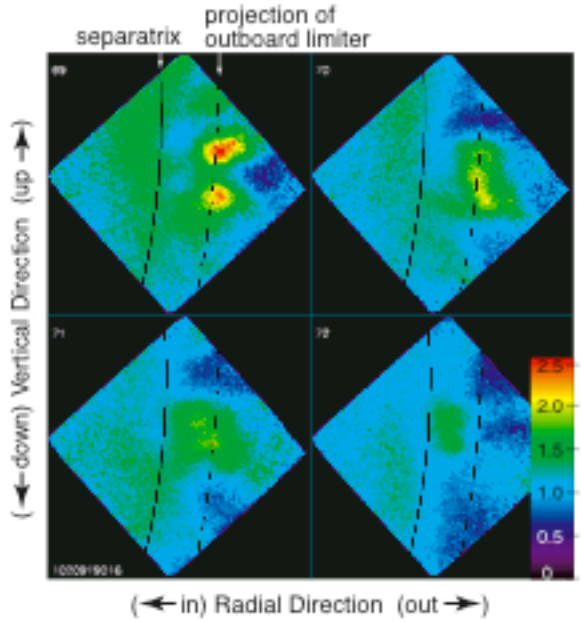
separatrix
projection of
outboard limiter
(down) Vertical Direction (up)
(in) Radial Direction (out)
2.5
2.0
1.5
1.0
0.5
0

Fig. 3

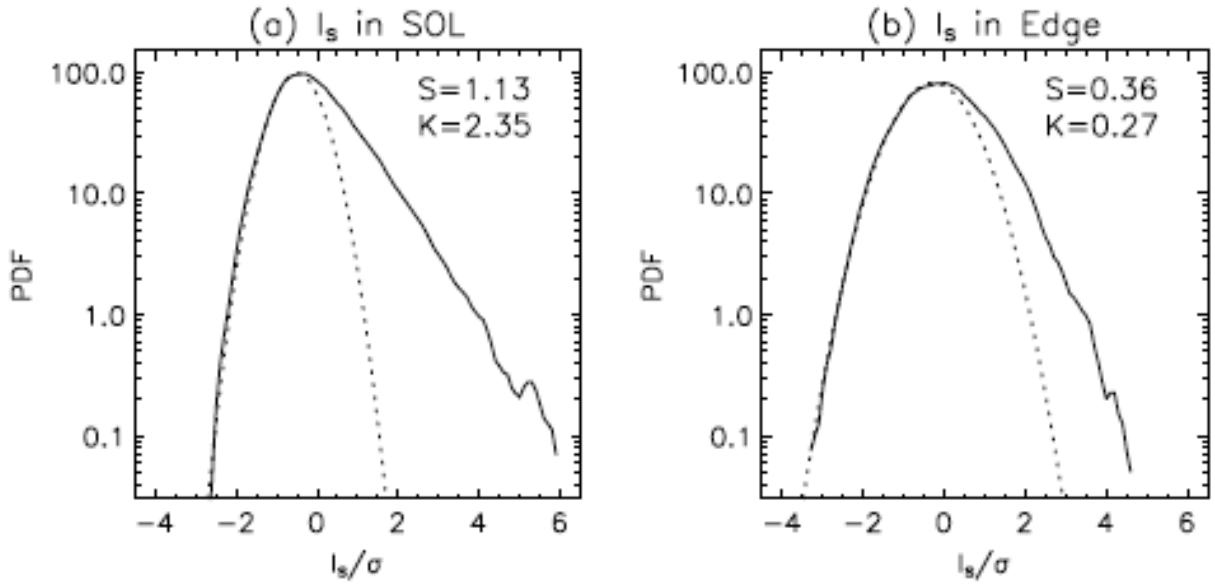
(a) I_s in SOL
S=1.13
K=2.35
PDF
100.0
10.0
1.0
0.1
−4
−2
0
2
4
6
I_s/σ
(b) I_s in Edge
S=0.36
K=0.27
PDF
100.0
10.0
1.0
0.1
−4
−2
0
2
4
6
I_s/σ

Fig. 4

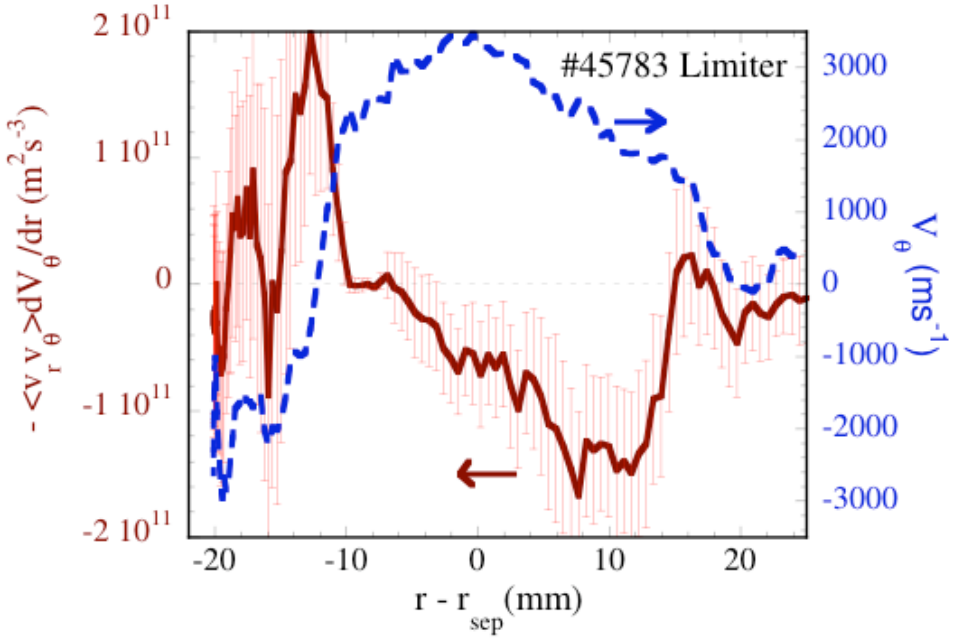
#45783 Limiter
2 10^11
1 10^11
0
-1 10^11
-2 10^11
3000
2000
1000
0
-1000
-2000
-3000
-20
-10
0
10
20
r - r_sep (mm)
- <v_r v_θ>dV_θ/dr (m^-2 s^-3)
V_θ (ms^-1)

(a)

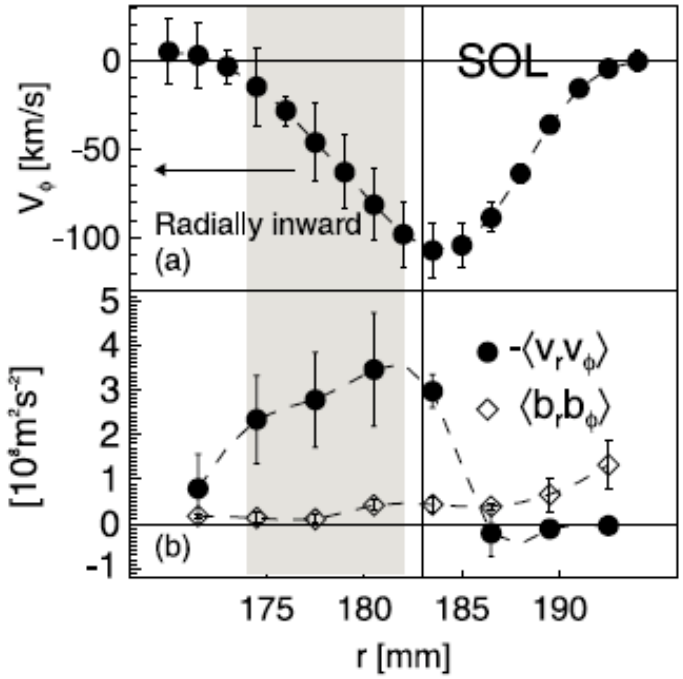
SOL
V_φ [km/s]
0
-50
-100
Radially inward
(a)
[10^4 m^2 s^-2]
5
4
3
2
1
0
-1
-⟨v_r v_φ⟩
⟨b_r b_φ⟩
(b)
175
180
185
190
r [mm]

(b)

Fig. 5

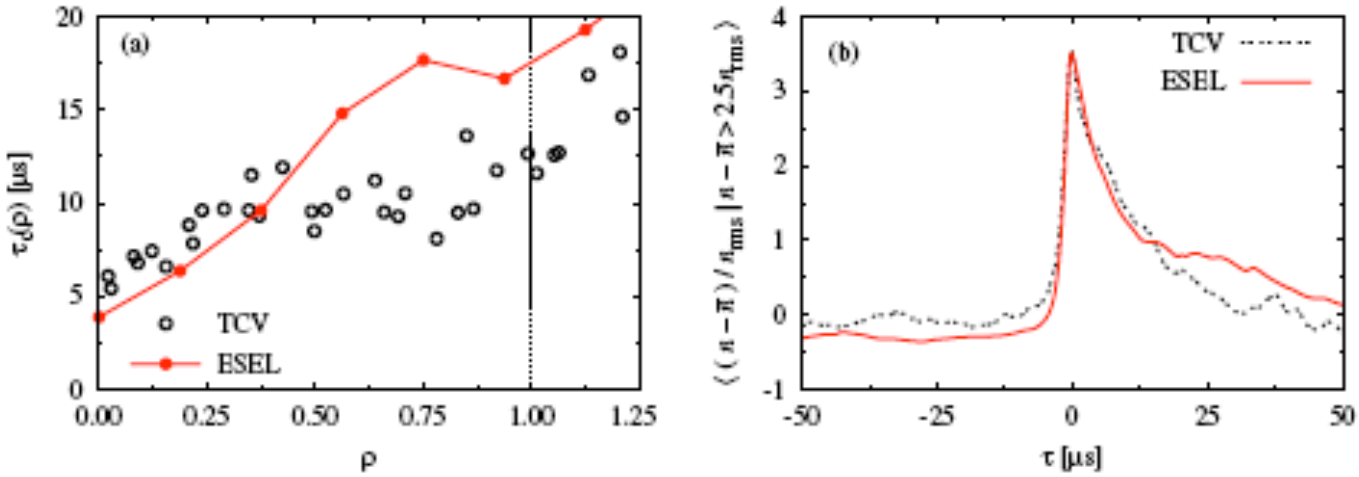
(a)
TCV
ESEL
$\tau_d(\rho)$ [μs]
ρ
(b)
TCV
ESEL
$\langle (n-\bar{n})/n_{rms} \mid n-\bar{n} > 2.5 n_{rms} \rangle$
τ [μs]

Fig. 6

The Princeton Plasma Physics Laboratory is operated
by Princeton University under contract
with the U.S. Department of Energy.

Information Services
Princeton Plasma Physics Laboratory
P.O. Box 451
Princeton, NJ 08543

Phone: 609-243-2750
Fax: 609-243-2751
e-mail: pppl_info@pppl.gov
Internet Address: http://www.pppl.gov